Materials Physics and Mechanics 24 (2015) 347-358 Received: November 3, 2015

SHOCK-INDUCED STRUCTURES IN COPPER

Yu. I. Meshcheryakov[1*], N.I. Zhigacheva[1], A. K. Divakov[1], G.V. Konovalov[1],

B.K. Barakhtin[2], S.V. Razorenov[3,4], O.V. Vyvenko[5], A.S. Bondarenko[5], I.V. Khomskaya[6]

[1]Institute of Problems of Mechanical Engineering RAS, Saint-Petersburg, Russia

[2]Central Institute of Constructional Materials "Prometei", Saint-Petersburg, Russia

[3]Tomsk State University, Russia,

[4]Institute of Problems of Chemical Physics RAS, Chernogolovka, Russia

[5]Saint-Petersburg State University, Russia,

[6]Physics of Metals Institute RAS, Ekaterinburg, Russia

*e-mail: ym38@mail.ru

Abstract. Shock loading of M3 copper within strain rate range of $5\cdot10^6$-$5{,}7\cdot10^6$ s^{-1} reveals a nucleation of structural objects of 5-30 μm in diameter, which present the three dimensional frameworks composed from shear bands of 50-200 nm spacing. The structures are shown to be nucleated by means of interference of longitudinal and periphery release waves. Transition of the material into structure unstable state responsible for the shear banding happens when rate of change of the velocity variance at the mesoscale becomes higher than the rate of change of the mean particle velocity. The sites of nucleation of 3D-structures are speculated to be the staking faults generated under action of chaotic velocity pulsations relevant to dynamic deformation. The physical model for formation of 3D-structures takes into account the intersection of the partial dislocations and Lomer - Cottrell barriers.

1. Introduction

Despite extensive research work on response of copper on shock loading many aspects of shock-induced structure formation in this material remain largely unknown. Specifically, it concerns to formation of localized 3D-structures at the mesoscale [1]. Some years ago we found that during the shock loading of M3 copper within narrow strain rate range of $5\cdot10^6$-$5.7\cdot10^6$ s^{-1} the 3D-formations of 5-30 μm in diameter are nucleated. In Fig. 1 the optical metallography of initial state of copper structure and its state after shock loading at the impact velocity of 500 m/s is presented. One can see the numerous black formations inside the grains (see Fig. 1b,c) which under higher magnification in the SEM-image look as chaotically distributed orthogonal networks of shear bands (Fig. 1d). Each network is composed from the shear bands of 50-100 nm spacing. Morphological features of the formations indicate on crystallographic mechanism of their nucleation whereas a positive correlation between dimensions of structures and strain rate allows to consider them as "domains of localized deformation" or 3D-structures.

In the present study, the results of further study of dynamic deformation and fracture of copper is presented. The investigations include: (i)) shock tests of plane targets under uniaxial strain conditions which allows to reveal the mechanisms of interference of shock and release waves resulting in nucleation of 3D-structures, (ii) exploring the nucleation of 3D-structures depending on the strain rate, (iii) investigation of morphology of 3D-structures by using

optical, SEM, TEM microscopy and EBSD-analysis, and (iv) development of physical model for the nucleation and growth of 3D-structures.

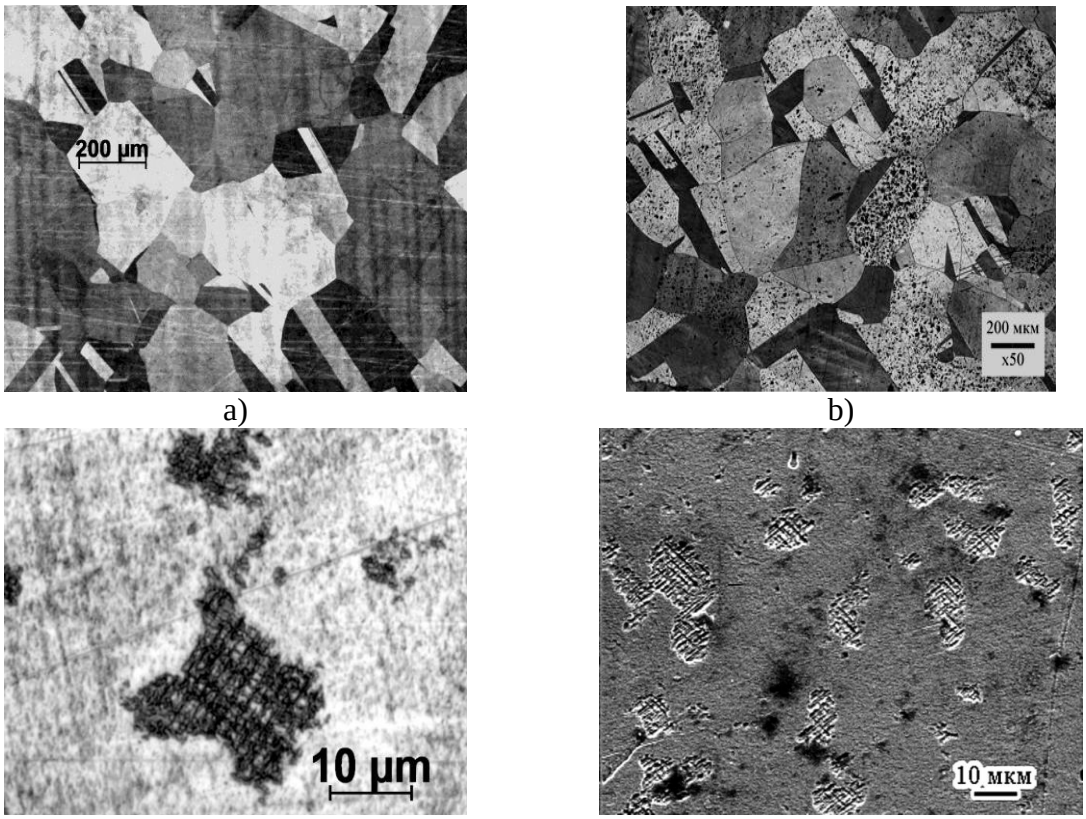

Fig. 1. Initial state of copper (*a*) and after loading at the impact velocity of 500 m/s (b-d).

2. Experiment

Shock tests of copper specimens were performed under uniaxial strain conditions by using (i) the one-stage 37 mm bore-diameter light gas gun and (ii) explosive lens. Two-channel velocity interferometer allows to register the free surface velocity and velocity variance at every shock loading. Typical free surface velocity profile is presented in Fig. 2.

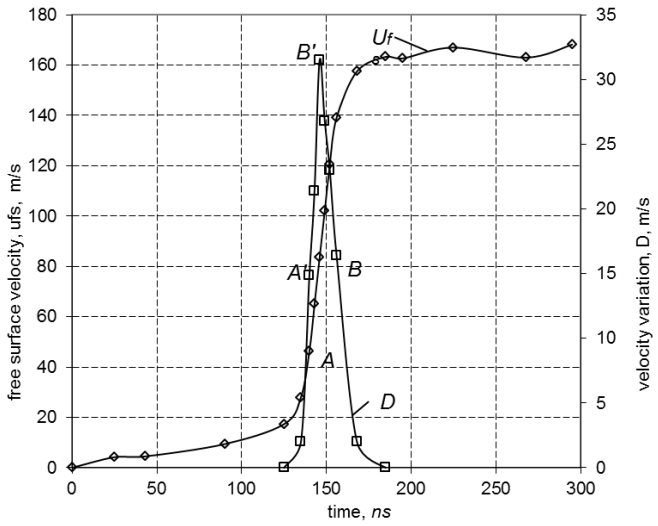

Fig. 2. Free surface velocity profile for the steady wave in 6 mm M3 copper target loaded at the impact velocity of 170,4 m/s.

This profile corresponds to steady shock wave in which the velocity variance maximum coincides with the middle of plastic front. Owing to precise focusing the laser beam of interferometer (diameter of laser spot at the free surface of target equals ~ 60 μm) all above characteristics should be attributed to mesoscale.

In the present experiments, the following characteristics of response of material on impact are registered: (i) dynamic yielding, Y, (ii) defect of the velocity at the plateau of compressive pulse, U_{def} , (iii) threshold of structural instability, U_{inst}, (iv) velocity variance, D, and (v) spall strength of material in the form of pull-back velocity, U_{pb}.

Enumerated characteristics are shown in Fig. 3 where the free surface velocity profile for 6 mm M3 copper target loaded at the impact velocity of 391 m/s is presented. The maximum value of the free surface velocity registered with interferometer equals 172 m/s. This supposes that the velocity defect achieves the value of $U_{def} = U_{imp} - U_{fsmax} = 219$ m/s.

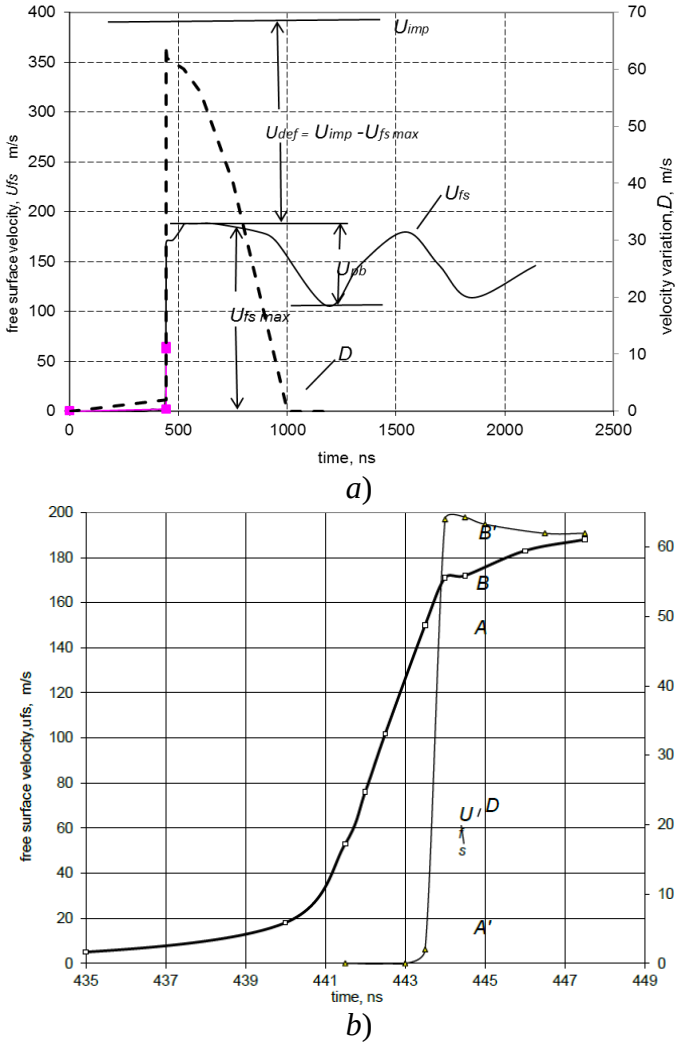

Fig. 3. Unsteady free surface velocity profile, U_{fs}, and velocity variance profile, D, for 6 mm M3 copper target loaded at the impact velocity of 391 m/s (a); the same in extended time scale (b).

The origin of defect of particle velocity is directly related to transition from evolutional to catastrophic regime of micro-macro momentum and energy exchange. Physically, breakdown of the free surface velocity means that kinetic energy of medium obtained from external loading goes on swinging the large-scale fluctuations (particle velocity pulsations). The criterion for transition from evolutional to catastrophic regime of momentum and energy

exchange between mesoscale and macroscale has the following form [1]:

$$\left(\frac{D}{u}\frac{\dot{D}}{\dot{u}}\right)\geq 1. \qquad (1)$$

Here D and u are the particle velocity variance and mean particle velocity, respectively, $\dot{D}$ and $\dot{u}$ are their time derivatives. Condition (1) asserts that the transition occurs if the particle velocity variance grows faster than the mean particle velocity. As a rule, the transition is accompanied by structural heterogenization of deformed material.

In case of shock-deformed solid, the components of criterion (1) are measurable values which can be inferred from the velocity profiles [2, 3]. Specifically, as example, let us apply the criterion (1) for the velocity profiles shown in Figs. 2 and 3 using the most steep sections of profiles *AB* and *A'B'*. For the impact velocity of 170.4 m/s (Fig. 2) one obtains: $D/u = 0.377$, $\dot{D}/\dot{u} = 0.531$ and $D/u\,(\dot{D}/\dot{u}) = 0.2$, so the criterion (1) is not fulfilled. In order to perform the same procedure for the unsteady velocity profile (Fig. 3*a*), the profile is extended in time (see Fig. 3*b*). Then for the impact velocity of 391 m/s one obtains: $D/u = 0.378$, $\dot{D}/\dot{u} = 2.97$ and $D/u\,(\dot{D}/\dot{u}) = 1.12 > 1$, so the criterion (1) is fulfilled.

In this case, the particle velocity profile suffers a breakdown, and velocity defect equals U_{def} = 219.6 m/s. Note that ratios D/u for both cases are practically equal each other, which coincides with the results of MD simulation in [4]. In the quoting work, two regimes of shock wave propagation in M2 copper correspond to different impact velocities, 89 m/s and 250 m/s. The first impact velocity corresponds to laminar regime of dynamic deformation whereas the second – to turbulent regime. In both cases, the ratio D/u turns out to be identical so it has been concluded that this ratio is not responsible for the transition of material from laminar to turbulent regime of dynamic straining. On the other hand, above calculations based on application of criterion (1) to real shock-wave experiments in the present study shows that the principal role in the transition plays the ratio $\dot{D}/\dot{u}$, that is the relationship between rates of change of the velocity variance and mean particle velocity.

In Table 1 the results of shock loading the M3 copper within impact velocity range of 170 – 500 m/s are provided. For obviousness, these data are also presented in Fig. 4 in the form of dependencies of pull-back velocity, velocity defect and HB-hardness on the impact velocity. It should be noted that increase of both the velocity defect and hardness begins at the impact velocity of 310 m/s and simultaneously the spall strength increases approximately by 20 %.

Table 1. Macroscopic response of M3 copper on impact.

Impact velocity, m/s ±0.5 %	170.4	231.9	319.6	391	467
Velocity defect, m/s ±0.5 %	0	7.4	24.6	219	328
Pull-back velocity, m/s ±0.3 %	72	73.7	105	107	109
HB-hardness, MPa ±4 %	67.5	73.6	90.5	90.5	94.5

In order to reveal a nature of 3D-structures, the shock loading of plane targets of 52 mm in diameter and 5-10 mm thickness was carried out in three schemes (Fig. 5*a-c*). In the first and third schemes of shock loading, the free surface of target could be monitored with the velocity interferometer to register the free surface velocity and velocity variance.

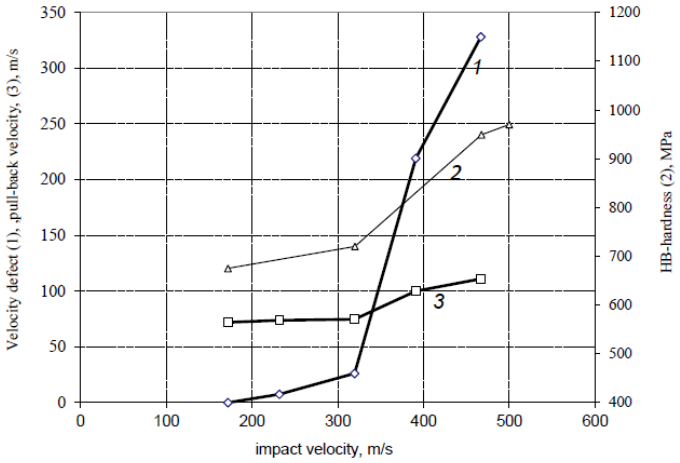

Fig. 4. Dependences of velocity defect (*1*), HB- hardness (*2*) and pull-back velocity (*3*) on the impact velocity.

Loading on scheme Fig. 5*a* provides an interference interaction of release wave reflected from the free surface of target and periphery release wave coming from side regions of the target. In the second scheme (Fig. 5*b*) the specimen was pressed inside the disk from the same material as a target. This excludes a passage of periphery release waves from side to central region [5]. In order to create the conditions for artificial spallation, a 2 mm copper plate was joined to the free surface of target. This scheme provides the conditions for single passage of shock wave through the specimen. In the third scheme (Fig. 5*c*), the additional plate was not joined to the free surface of target so the release wave reflected from the free surface propagates back into body of the target whereas the periphery release wave is detained.

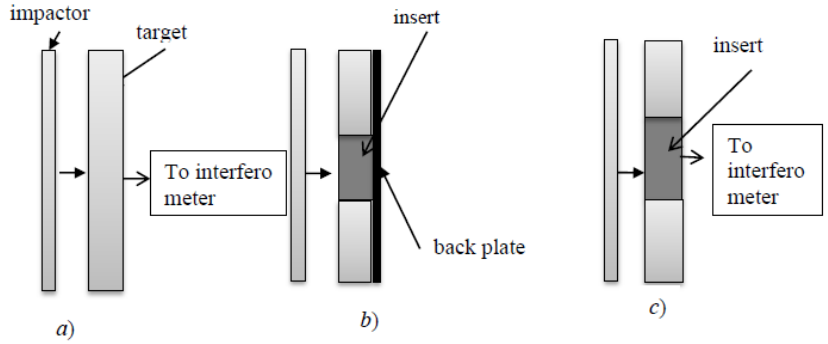

Fig. 5. Schemes of shock loading.

In Fig. 6 the range of impact velocities where 3D-stuctures are nucleated is presented. Dependence of hardness on the impact velocity is provided as well. One can see a coordinated behavior of density of 3D-structures and macroscopic strength of material. This means that 3D-structures are the objects, which strengthen the material. This assertion was checked in special shock tests in which after first loading on scheme Fig. 5*a* at the impact velocity of 398 m/s the additional shock loading at the impact velocity of 170 m/s has been performed. The free surface velocity profiles obtained after single and double shock loadings are presented in Fig. 7. One can see that repeated shock loading reveals the increase of the elastic precursor, *Y*, by 10-12 times and macroscopic viscosity by 3-5 times. The increase of dynamic yield limit proves to be the greater, the higher velocity of the first loading. At the same time, the spall strength of material, *W*, did not change – pull-back velocities for both profiles turned out to be equaled each other. This means that spall-strength which characterizes the tension strength of composite material (matrix plus 3D-structures) is determined by the matrix.

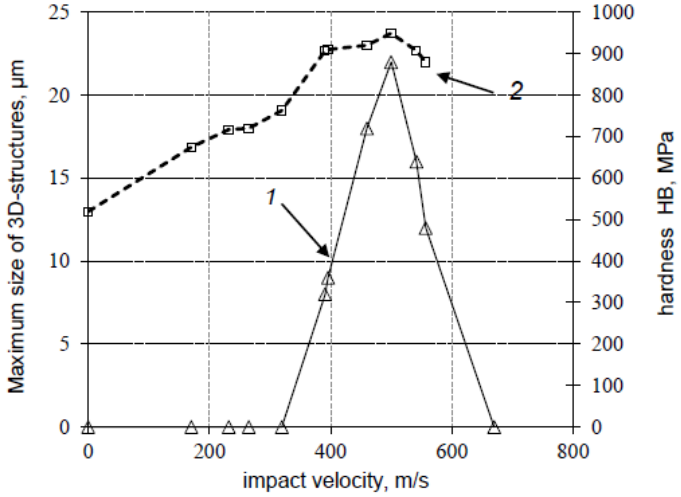

Fig. 6. Dependencies of mean size of 3D-structures (1) and HB-hardness (2) on the impact velocity.

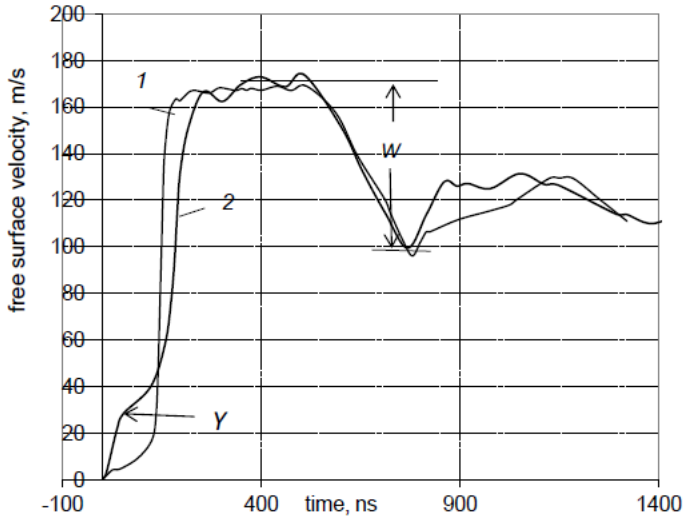

Fig. 7. The velocity profiles in M3 copper after single (*1*) and double (*2*) shocks.

4. Microstructure investigations

In order to reveal the structure of "deformation domains" and understand the mechanism of their nucleation, the microstructural investigations were carried out by using the optical microscopes Neophot-32, Axio Observer Z-1, scanning microscope Philips SEM-535 and EBSD-analysis of post-shocked specimens. The state of microstructure proves to depend on the scheme of shock loading. In the first scheme of loading, there is a reflection of shock wave from the free surface of target and propagation of release wave back into target. Herewith, in the region of target under impactor, the release wave propagating from the free surface interacts with the periphery release wave propagating from the side region of target. Just in this scheme the 3D-structures are nucleated. The dynamic deformation under uniaxial strain conditions is known to be characterized by the summary action of hydrostatic pressure and deviator component of stress. The deviator component sensitively depends on the orientation of grain with respect to applied stress, which, in turn, is determined by the shock wave propagation direction and Schmid-factor. The 3D-structures are nucleated only in the grains which are properly oriented with respect to wave propagation direction and where the value of shear stress is sufficient for nucleating the shear bands. This is seen in Fig. 8 where the grains of two different orientations of sliding planes are presented. In the upper grain (A)

the shear bands are oriented in single direction whereas in the bottom grain (B) the 3D-structures consist of two mutual perpendicular families of shear bands. In the second case, the sliding planes are oriented approximately under 45° with respect to the wave propagation direction so the families of orthogonal shear bands are nucleated in two directions.

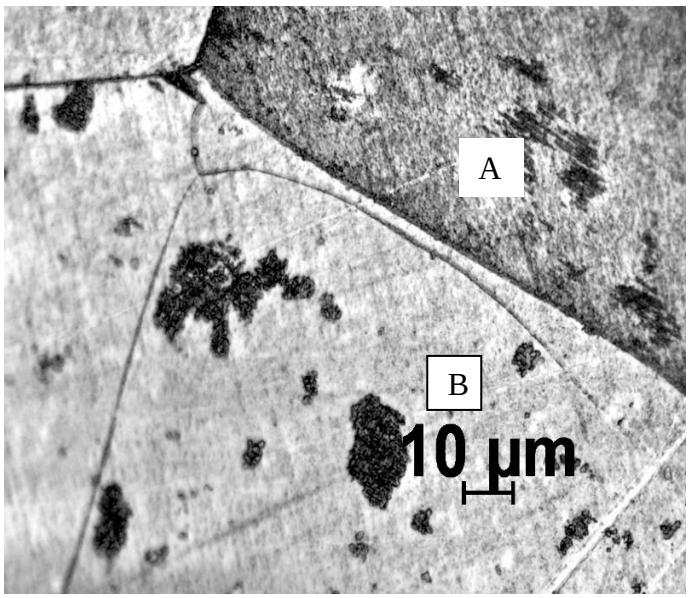

Fig. 8. Micrograph of the 3D-structures in the grains of different orientation (a), boundary fracture of spesimen loaded in scheme 3*c* (b).

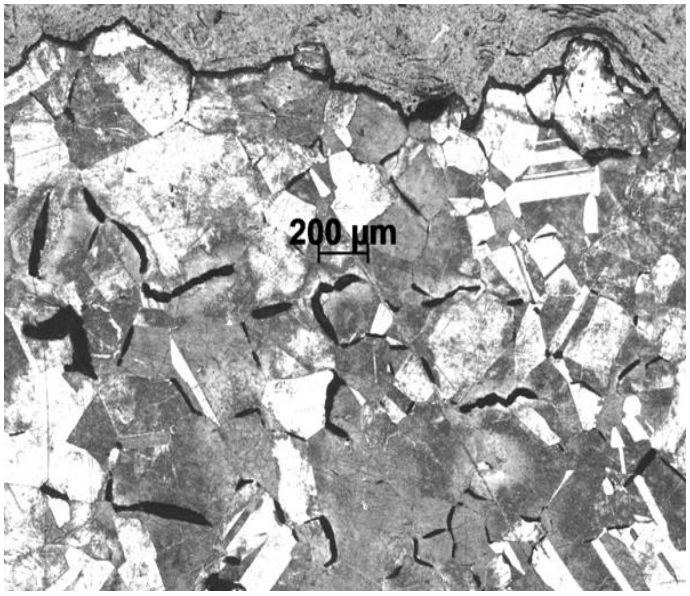

Fig. 9. Fracture along the grain boundaries of specimen loaded in scheme 3*a*.

In the scheme Fig.5*b* which provides the conditions for single passage of shock wave through the specimen, the 3D-structure are not nucleated, so the micrograph pattern looks as in initial state (Fig. 1*a*).

In the third scheme of shock loading, the additional plate at the back side of target was not joined (Fig. 5*c*). In this case, the release wave from the free surface of target propagates from back side to loaded surface although the periphery release waves are suppressed. Deformation and fracture of the material flow only along the grain boundaries whereas the volume of grains remains to be free from the 3D-structures (Fig. 9).

Thus, it may be concluded that 3D-structures are formed only during the interference of longitudinal and periphery release waves propagating from back and side surfaces of target. Herewith, hardness of post-shocked specimens without 3D-structures turns out to be smaller than the hardness of specimens containing these structures. For example, when loaded at the impact velocity of 500 m/s in the scheme Fig. 5*a*, the copper target shows the HB-hardness equaled to 950 MPa whereas after loading in the scheme Fig. 5*b* when the 3D-structures are absent, the HB-hardness equals 760 MPa.

The second parameter of shock loading which determines the characteristics of 3D-structures is the duration of loading pulse. The additional set of experiments has been performed with the so-called explosive lens (Fig. 10). This instrumentation provides the shock loading with the three-angle stress pulse of large duration. In our experiments, the aluminum plate of 2 mm thickness was accelerated to the velocity of 650 m/s. In Fig. 11*a*) the micrograph of structure in post-shocked specimen after shock loading with the explosive lens is presented. The duration of load stress pulse herein is approximately five times greater as compared to load pulse initiated with the light gas gun. In this case, 3D-structures are also nucleated only in the properly oriented grains but dimensions of 3D-sructures are much greater so they separated from each other by the narrow bands of 10 nm width. In Fig. 11*b* the TEM-image of the shear bands constituting the 3D-formation is presented.

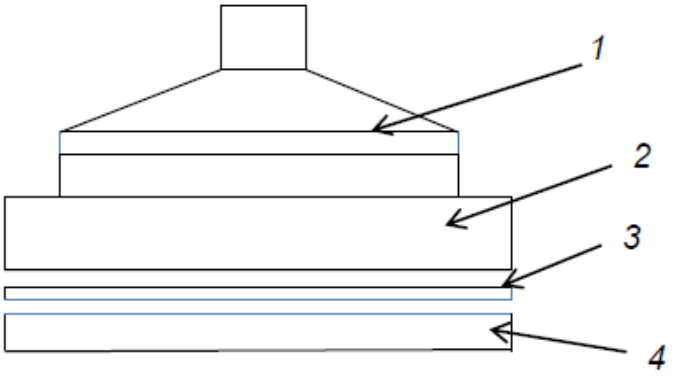

Fig. 10. Scheme of shock loading with explosive lens. 1 – explosive, 2 – thick plate-attenuator, 3 – laying of low-impedance material, 4 – plate-impactor.

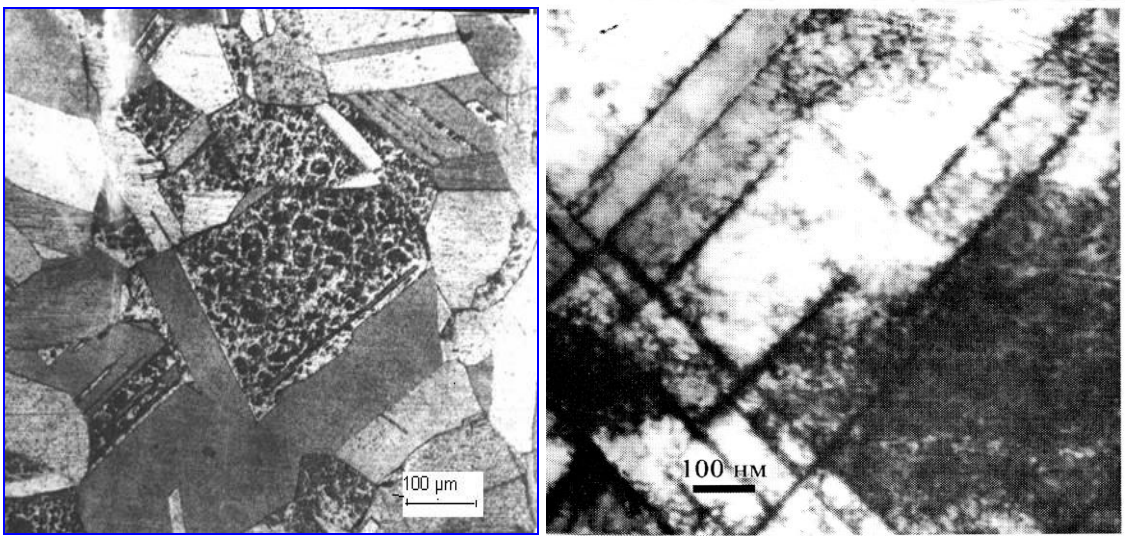

a) *b*)

Fig. 11. Micrograph of structure after shock loading in scheme Fig. 3*a* by using the explosive lens (*a*), TEM – pattern of this structure (*b*).

Complex of microstructural investigations shows that "deformation domains" are the 3D frameworks composed from the shear bands of 50-200 nm spacing. All the shear bands are attached to the plane system {111} and are the groups of partial dislocations Shockley which are linked with stacking fault. In fcc-lattice, the such crystalline defects can slide in planes {111} in closed packed directions <011>.

Beside the optical, SEM and TEM investigations of post-shocked specimens, EBSD-analysis was performed in several regions of targets. In Figs. 12 and 13 two EBSD- patterns corresponding different points of specimen are presented. Comparison of EBSD- patterns from the 3D-structure (indicated by symbol *A* in Fig. 11) and from the place which is free from 3D-structures (symbol *B* in Fig.12) shows that the EBSD-patterns are identical. Thus, it can be concluded that 3D-structures are coherent with the lattice of grain and doesn't change the crystallography of grain.

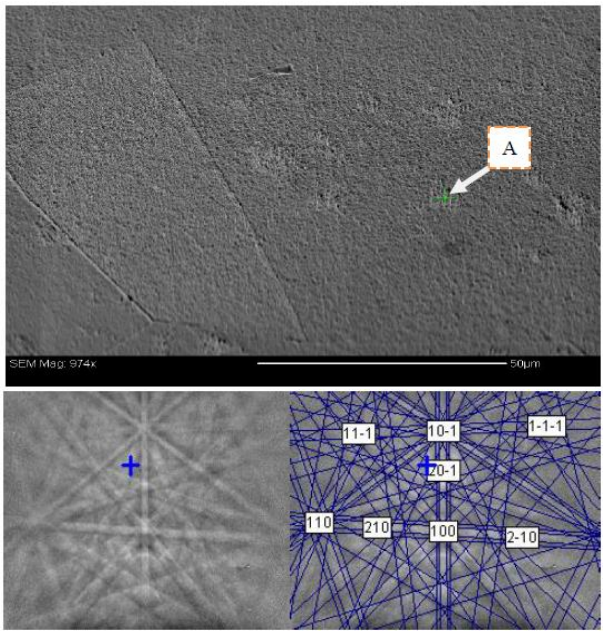

Fig. 12. EBSD- pattern from center of 3D structure.

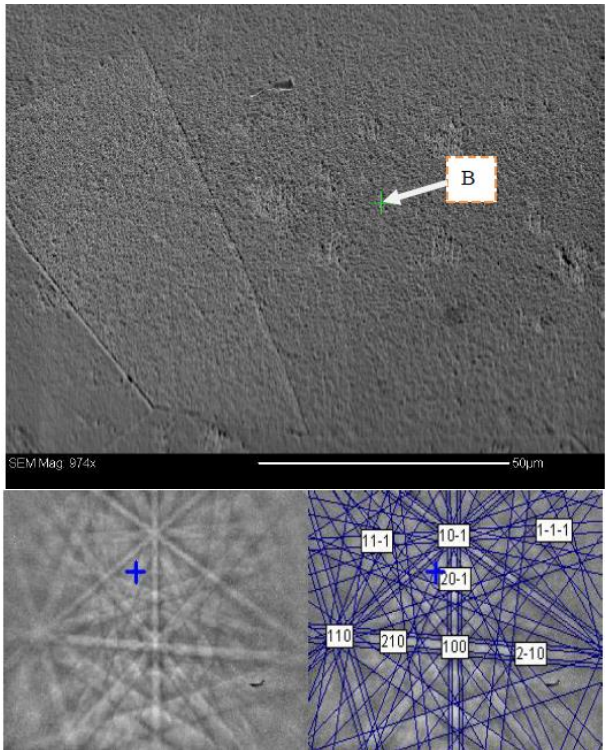

Fig. 13. EBSD- pattern from the same grain outside the 3D structures.

5. Physical model for 3D-structure

On the basis of microstructural studying a following sequence of shock-induced structural changes in M3 copper may be suggested.

Stage 1. Under conditions of shock loading, upon first passage of shock wave, a high density of crystalline lattice defects is nucleated. The majority of dislocations is presented by partial dislocations with stacking faults. The mechanisms of nucleation of stacking faults during dynamic deformation of copper have been analyzed in [6]. The threshold value of shear stress necessary for nucleation of stacking fault was found to be equaled to Hugoniot elastic limit which in the case of copper equals approximately 0,01 GPa.

Experimental and theoretical studies of dynamic straining show that one of basic mechanisms of momentum and energy transportation from scale level to another under conditions of multiscale dynamic deformation is the pulsations of particle velocity [1]. The quantitative characteristic of the velocity pulsations is the particle velocity variance at the mesoscale (in West literature the mesoscale pulsations call a "granular temperature").

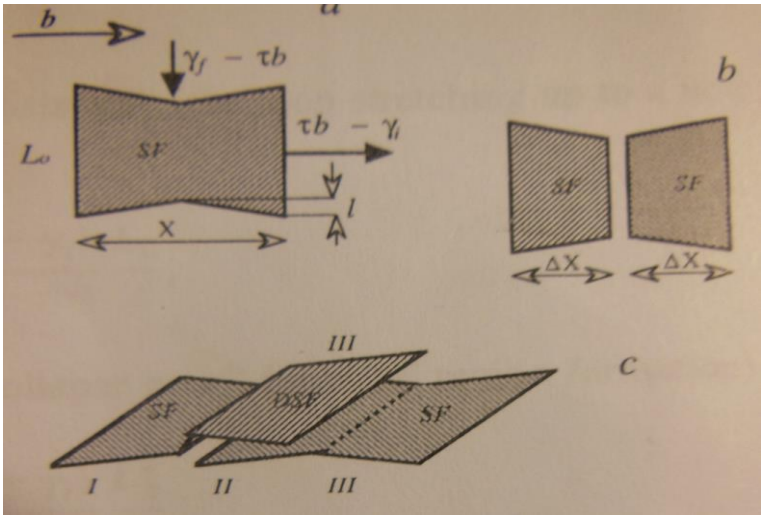

Fig. 14. Mechanism of growth and multiplication of stacking fault and partial dislocations (after [6]).

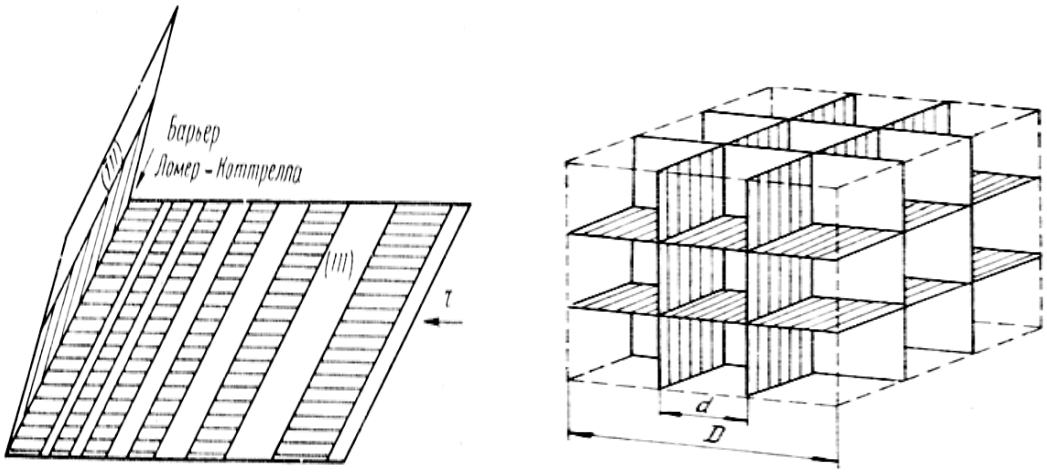

a) *b*)

Fig. 15. Scheme of forming the framework structure.

At the strain rate of $5 \cdot 10^6$ - $5.7 \cdot 10^6$ s^{-1} the particle velocity variance equals ~ 65 m/s (see Fig. 3). It suggests an existence of amplitude throws of velocity pulsations up to 90 ÷ 100 m/s, which corresponds to local stress of the order of 1.4 - 1.7 GPa. This value is much higher than threshold stress necessary for nucleation of stacking fault [6-8]. Thus, else at the first passage of shock front the chaotic pulsations can initiate a nucleation of stacking faults. Accordingly, a lot of partial dislocation are nucleated around the stacking faults during the first passage of shock wave. The mechanism of nucleation and growth of partial dislocations is qualitatively shown in Fig. 14.

Stage 2. Upon propagation of release wave from the free surface back into target, the local stresses relax due to motion of partial dislocations. In fcc-crystals, under contrary motion of partials, the new defects are formed in crossed slide planes, so-called ”sitting” Lomer-Cottrell dislocations, which play a role of barriers for other sliding dislocations [9-11] (see Fig. 15). The families of partials together with Lomer-Cottrell barriers form the three dimensional frameworks of shear bands (deformation domains). Chaotic distribution of deformation domains in grains is, firstly, a sequence of random positions of stacking faults during the first passage of shock front and, secondly, random positions of Lomer-Cottrell barriers. As a result, the material presents a composite consisting of matrix (fcc-lattice) and

chaotically distributed frameworks "frozen" into crystalline lattice. Herewith, the following deformation are not able to change their morphology. It is clearly seen in Fig. 16 where the 3D-structures are intersected with the shear bands initiated by the additional shock loading.

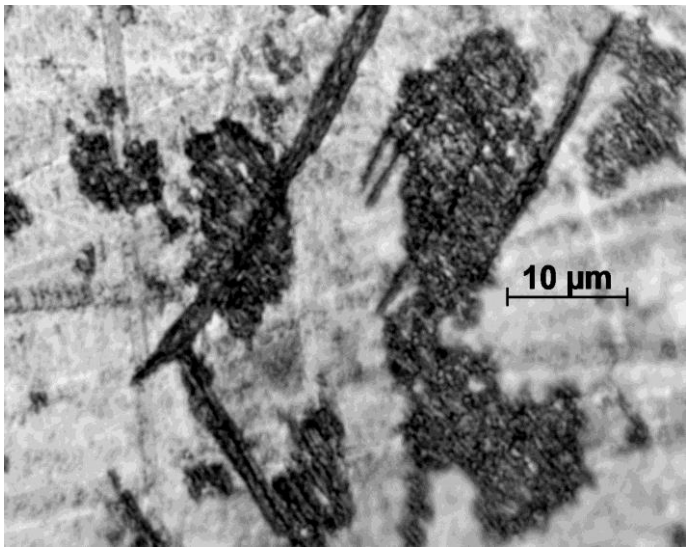

Fig. 16. Intersection of framework structures with the shear bands caused by the repeated dynamic deformation at the impact velocity of 540 m/s.

Described sequence of structural changing occurring under shock loading of copper corresponds to experimental data [12] obtained with the impulse X-ray scanning the shock deformed copper in real time. It is shown that in fcc-crystals the shear deformation is realized mainly by means of nucleation of stacking faults. Above results also agree with the results of MD-modeling [13] which shows that stacking faults in copper are spontaneously nucleated at early stages of high-velocity straining.

6. Conclusions

In summary, complex of investigations including different schemes of loading, interferometric registration of the free surface velocity and microstructural studying of post-shocked specimens, establish the following conclusions about shock-induced mesoscale formations in copper. First, the shock loading under different schemes of wave interaction give direct evidence that formations are the 3D-structures which are nucleated under interaction of longitudinal and periphery release waves. Second, as result of interaction, the families of partial dislocations form the three dimensional framework structures of shear bands. Herewith, multilayer structures ("deformation domains") are composed of partial dislocations and stacking faults fixed with "sitting" Lomer-Cottrel barriers. Third, the forming of "deformation domain" happens at the critical values of two dynamic characteristics of dynamic straining at the mesoscale: (i) rate of change of the velocity variance and (ii) rate of change of mean particle velocity. Transition into structure unstable state is shown to happen when rate of change of the velocity variance becomes higher than the rate of change of mean particle velocity.

Acknowledgments

This work is performed with using the equipment of Resource Center "Nanotechnologies" at Saint-Petersburg State University.

Financial support from Saint Petersburg State University research grant 6.37.671.2013 is acknowledged.

References

[1] Yu.I. Meshcheryakov, A.K. Divakov, N.I. Zhigacheva, I.P. Makarevich, B.K. Barakhtin // *Physical Review B* **78** (2008) 64301.
[2] J.R. Asay, L.M. Barker // *Journal of Applied Physics* **48** (1974) 2545.
[3] Yu.I. Meshcheryakov, A.K. Divakov // *Dymat Journal* **1** (1994) 271.
[4] K. Yano, Y-Y. Horie // *Physical Review B* **59** (1999) 13672.
[5] W.F. Hartman // *Journal of Applied Physics* **35** (1964) 2090.
[6] E. Zaretzky // *Journal of Applied Physics* **78** (1995) 3740.
[7] P. Jongenburger // *Acta Metallurgica* **11** (1963) 992.
[8] A. Coujou // *Acta Metallurgica* **31** (1983) 1505.
[9] K. Rayan // *Scripta Metallurgica* **17** (1983) 101.
[10] I.I. Novikov, *Defects of crystals in metals* (Metallyrgy, Moscow, 1975).
[11] V.F. Moiseev, V.I. Trefiliv, In: *Strain hardening and destruction of polycrystalline metals*, ed. by V.I. Trefiliv (Naukova Dumka, Kiev, 1989), p. 7.
[12] E.B. Zaretsky, G.I. Kanel, M.A. Mogilevsky, V.E. Fortov // *High Temperature Physics* **29** (1991) 1002.
[13] M.A. Mogilevsky, In; *Shock Waves and High Strain Rate Phenomena in Metal*, eds. M.A. Meyers and L.E. Murr (Plenum Press, N.Y., 1981), p. 531.